ELSEVIER

Materials Science and Engineering A233 (1997) 15–25

MATERIALS SCIENCE & ENGINEERING A

In situ high-voltage electron microscope deformation study of a two-phase ($\alpha_2 + \gamma$) Ti–Al alloy

D. Häussler [a,*], U. Messerschmidt [a], M. Bartsch [a], F. Appel [b], R. Wagner [b]

[a] *Max Planck Institute of Microstructure Physics, Weinberg 2, Halle, D-06120, Germany*
[b] *Institute of Materials Research, GKSS-Research Centre, Geesthacht, D-21502, Germany*

Received 17 September 1996; received in revised form 28 January 1997

Abstract

In situ straining experiments in a high-voltage electron microscope have been performed on two-phase Ti-47at.%Al-2at.Cr-0.2at.%Si at room temperature and at 900 K. Two microstructures were investigated which were produced by thermomechanical treatments: a so-called near-gamma and a nearly lamellar microstructure. The processes controlling the motion of individual dislocations in the γ phase are very similar in both materials. At room temperature, ordinary dislocations and superdislocations show a jerky motion which is impeded by localized obstacles and jogs. At high temperature, the dislocations are smoothly bent or arranged in preferred orientations and move in a viscous way. This mode of motions as well as the nonplanar arrangement of dislocations point to the action of climb as an essential process during the high-temperature deformation of Ti–Al. These observations are very similar to those on Al-rich single phase TiAl investigated earlier. The considerably higher flow stress of the two-phase alloys is an effect of their particular microstructures, i.e. of grain boundaries and lamella interfaces. © 1997 Elsevier Science S.A.

Keywords: Thermomechanical treatment; Lamella interfaces; Microstructures; Titanium aluminides

1. Introduction

Titanium aluminides are prospective materials for structural application because of their light weight, relatively good corrosion resistance and particularly because of the high flow stresses for temperatures as high as about 1100 K . The extraordinary strength properties of alloys near the TiAl composition may show an anomalous temperature dependence of the flow stress for aluminium concentrations exceeding 50%, while titanium-rich materials exhibit a broad plateau-region under the same conditions. However, like many other intermetallic materials, titanium aluminides lack damage tolerance at ambient temperatures, which limits practical application. In this respect, significant improvement can be achieved in titanium-rich alloys which contain the intermetallic phases α_2 (Ti_3Al) and γ (TiAl). Due to microalloying with ternary elements like Cr, Mn, Nb, Si and B, an optimisation of the microstructure with reasonable tensile ductility and fracture toughness were realized so that the materials are now seriously being considered for engineering applications in turbine engines (for a recent review see [1]). Regardless of the effect of the microstructure the superior strength properties of the two-phase alloys may be attributed to several aspects of dislocation dynamics. The factors concerned are interface related deformation phenomena [2,3] and the increase of dislocation mobility in the γ phase due to the impurity gettering ability of the α_2 phase [4]. Direct information on these processes is rare, but is expected to be helpful for further alloy design.

The dynamic behaviour of dislocations can well be observed in in situ straining experiments in a transmission electron microscope. Respective studies on single-phase γ material have been performed in a 200 kV electron microscope [5–7] as well as in a high-voltage electron microscope (HVEM) [8–10]. While the flow stress anomaly of single phase alloys can quite easily be

* Corresponding author. Tel.: +49 345 5582921; fax: +49 345 5511223.

PII S0921-5093(97)00044-0

understood in terms of superdislocations of a Burgers vector $\vec{b} = \langle 101 \rangle$ [11], the in situ experiments show a dominance of ordinary dislocations with $\vec{b} = \frac{1}{2}\langle 110 \rangle$ Burgers vectors, in accordance with some conventional electron microscope results. Particularly the experiments in [8–10] show a dynamic behaviour of dislocations most different at room temperature and at high temperatures. At room temperature, the curly shape of dislocations and their jerky motion seem to indicate that the mobility of both ordinary dislocations and superdislocations is mainly controlled by precipitation hardening, i.e. by an extrinsic mechanism. It is quite probable that the glide obstacles are small precipitates in the form of TiO or alumina, 'H-phase' as well other ternary phases [12], but their nature has not yet been determined unequivocally. At deformation temperatures of about 900 K, ordinary dislocations are smoothly bowed in non-planar arrangements and move in a viscous manner. This points to the importance of diffusion processes, probably climb. A similar conclusion had been drawn from high-temperature in situ annealing studies [13]. Superdislocations are aligned in preferred orientations as it is expected from their core structure. During in situ straining $1/6\langle 11\,\bar{2}\rangle\{111\}$ order twinning occurred at all temperatures, but its relative contribution to deformation could not be assessed. The results of the in situ experiments, particularly at high temperatures, help one understand the anomalous deformation behaviour of Ti–Al alloys, although a coherent theoretical picture has not yet evolved.

Plastic deformation of the technically more important two-phase materials mainly occurs in the γ phase. Thus, regarding the significant variation of strength properties with deviation from stoichiometry mentioned above, a comparison of the dislocation behaviour in the γ phase of aluminium-rich and titanium-rich alloys is of particular interest. Investigation of this problem is a subject of the present study. The two-phase alloy chosen is characterised by an improved strength and room temperature workability [14]. Depending on the thermomechanical treatment one of two microstructures may be produced, either a near-gamma structure or a nearly lamellar one, both having similar dependences of the flow stress as well as the strain rate sensitivity on temperature [15]. The mechanical properties of the two materials have been thoroughly tested and the microstructures are investigated by means of TEM [13–15]. As reported in many investigations [1,16–19], there are significant differences in the strength properties of near-gamma and nearly lamellar materials. In the present materials this becomes evident as follows. Among others, remarkable property relationships occur between both materials of complementary character [20]. The near-gamma microstructure exhibits the higher tensile fracture strain (2...4% instead of 0.5...1%) but the nearly lamellar microstructure shows the higher fracture toughness (20...24 MPa $m^{1/2}$ instead of 12...16 MPa $m^{1/2}$) [21]. In order to explain this inverse correlation between tensile ductility and fracture toughness, detailed investigations regarding the deformation and failure characteristics of the two microstructures have been performed [17,19–21]. Accordingly, the different mechanical properties have mainly been attributed to differences in crack nucleation and propagation. Nevertheless, various features of the toughening processes can be related to dislocation dynamics in the plastic zone of crack tips. Investigation of crack propagation in near-gamma and nearly lamellar microstructures is therefore another aspect of the present study.

In spite of the important influences of the particular microstructures on the deformation parameters [3,13–15,20–24], basic deformation properties as for example the flow stress anomaly, should be controlled by the dynamic behaviour of all types of dislocations. The present paper reports on an in situ transmission electron microscopy study of the two-phase alloys described above and compares the results with those of the single-phase γ material. In general, the results of the in situ experiments have to be interpreted with care owing to the limitations of the technique which arise from surface effects and radiation damage. Thus, the observations will be discussed and related to results obtained in the same materials by other experimental techniques.

2. Experimental

In situ straining experiments were performed on specimens prepared from castings of an $(\alpha_2 + \gamma)$ Ti–Al alloy of composition Ti-47at.%Al-2at.%Cr-0.2at.%Si. As discussed in the Section 1, two types of microstructures were produced by thermomechanical treatments. (1) A globular or so-called near-gamma microstructure of an average grain size of the order of 11 μm resulted from two-stage forging at 1500 K with a height reduction of 70% in each step. In this material, a small volume fraction of the α_2 phase is located at the grain boundary triple-nodes of the γ grains. (2) Starting from this state, annealing at 1650 K for 1 h caused a nearly lamellar microstructure consisting of lamellar colonies of about 300 μm in diameter, inside which γ lamellae of different orientations alternate with few α_2 lamellae of thicknesses between about 0.02 and 2 μm.

Micro-tensile specimens were prepared for in situ electron microscopy by cutting, grinding and two-step jet polishing between platinum masks using an electrolyte consisting of methanol, butanol and perchloric acid (233 K, 20 V). Usually, the central region of the strip-shaped specimens had got one hole with large transparent regions around it. In the target preparation

Fig. 1. Overview of the microstructure of near gamma Ti-Al during an in situ straining experiment. All grains are of the γ phase except the α_2 grains which are marked. The specimen contains a crack. Arrow, tensile direction

technique using etched surfaces, lamellae in the nearly lamellar microstructure were oriented edge-on, at the same time slightly inclined to the tensile axis. The specimens were mounted onto the grips of the quantitative straining stages for the high-voltage electron microscope, which are described in [25] for room temperature and in [26] for high temperatures, respectively. The present high-temperature experiments were carried out at about 900 K. The Jeol 1000 HVEM used was operated at 1000 kV. The deformation was performed in small load increments. The dislocation structures were recorded under full load on photographic film or video tape, respectively. In order to restrict unavoidable radiation damage, in their unloaded state the dislocation structures were characterised in detail in a wide-angle goniometer at room temperature.

Fig. 1 and Fig. 2 give a general view of the microstructures and of the shape of cracks in the near-gamma and nearly lamellar materials investigated, imaged at identical magnifications.

3. Results

The deformation behaviour at room temperature is described in Section 3.1, that at 900 K in Section 3.2. The dynamic properties of dislocations and twins are always characterised first and the description of the influence of the two types of microstructure on the behaviour of the dislocations follows. The final section Section 3.3 treats the nucleation and propagation of cracks in both microstructures at room temperature

Fig. 2. Overview of the microstructure of nearly lamellar Ti-Al during an in situ straining experiment. Most of the lamellae are of the γ phase. Foil normal $[101]_\gamma$. The specimen contains a crack. Crack faces are mainly {111}. Arrow, tensile direction

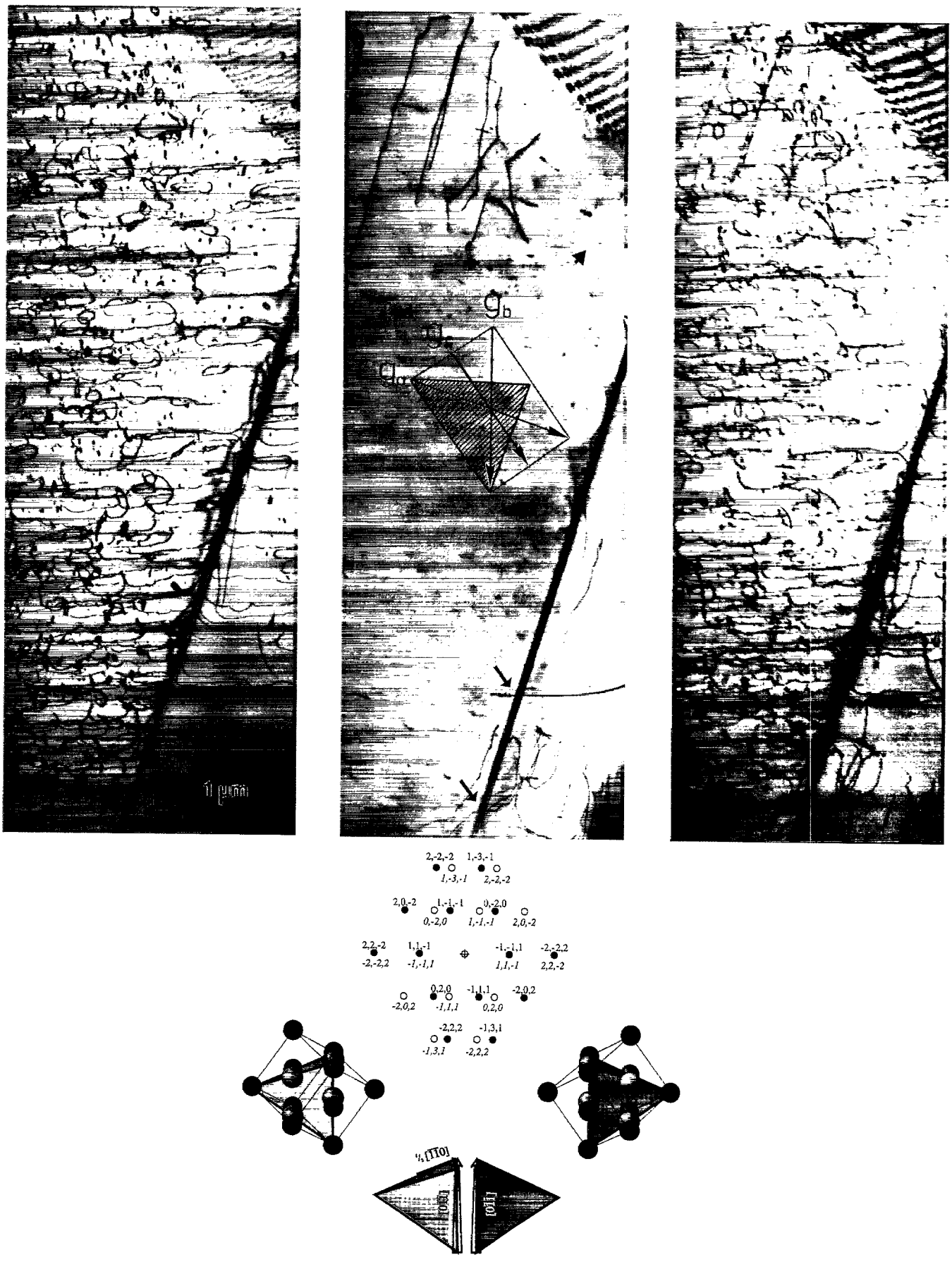
1 μm
g_b
2,-2,-2 1,-3,-1
1,-3,-1 2,-2,-2
2,0,-2 1,-1,-1 0,-2,0
0,-2,0 1,-1,-1 2,0,-2
2,2,-2 1,1,-1 -1,-1,1 -2,-2,2
-2,-2,2 -1,-1,1 1,1,-1 2,2,-2
0,2,0 -1,1,1 -2,0,2
-2,0,2 -1,1,1 0,2,0
-2,2,2 -1,3,1
-1,3,1 -2,2,2
[011]
[001]
[011]

Fig. 3.

and at 900 K.

In both the near-gamma as well the nearly lamellar microstructures deformation takes place mainly in the γ phase. Therefore, the following treatment deals with this main phase exclusively.

3.1. Deformation at room temperature

Fig. 3 displays ordinary dislocations with $\vec{b} = \frac{1}{2}[\bar{1}\ \bar{1}\ 0]$ and superdislocations with $\vec{b} = [0\ \bar{1}\ \bar{1}]$ which have moved and were recorded during straining of the near-gamma material. The figure gives an impression of the relative densities of ordinary dislocations and superdislocations, with ordinary dislocations dominating. The dislocations in Fig. 3(a–c) are mainly of screw character and glide on a single set of $(1\ \bar{1}\ 1)$ planes (see schematic drawing in Fig. 3(d)). The ordinary dislocations are pinned at and bowed-out between jogs and other obstacles at mean distances of about 0.15 μm along the dislocation line. Superdislocations are pinned in a similar way. They are, however, less bowed-out. Dislocation debris has been trailed by the moving dislocations, mainly by the ordinary dislocations with Burgers vector $\vec{b} = \frac{1}{2}[\bar{1}\ \bar{1}\ 0]$ (Fig. 3(a)), but occasionally also by superdislocations as indicated by arrows in Fig. 3(b). As the video recordings show, the dislocations move in a jerky way, get pinned again, bow out and produce a high density of debris.

The results were similar for materials of the nearly lamellar microstructure (Fig. 4, on the same scale as Fig. 3. The Thompson pseudo-tetrahedron ($c/a \cong 1.02$) inserted and other crystallographic indications regarding Fig. 4 are related to the widest lamella). The α_2 and γ phases forming the lamellar structure have the orientation relationship [27]

$$<1\ \bar{1}\ 0>_\gamma \| <1\ 1\ \bar{2}\ 0>_{\alpha_2} \text{ and } \{111\}_\gamma \| (0001)_{\alpha_2},$$

where the $\{111\}_\gamma$ plane is parallel to the lamellar boundaries. There is a random occurrence of six γ variants, which can formally be described by rotations of one lamella with respect to its neighbour by multiples of 60° about $\langle 111\rangle_\gamma$. Thus, in addition to the α_2/γ interface, three distinct types of γ/γ interfaces occur, which correspond to rotations of 60° (pseudo-twin relation), 120° (matrix/matrix relation) and 180° (true-twin-relation). With respect to the imaging direction $[\bar{1}\ 0\ \bar{1}]$ in Fig. 4, two orientations are possible for screw dislocations: parallel to the trace of the interface, or inclined to it, i.e. imaged at an angle of 61° related to the trace of the interface (see inset). The latter dislocations are characterised by $\vec{b} = [\bar{1}\ 0\ 1]$. Such dislocations appear in a high density. In addition to these superdislocations, ordinary dislocations of $\vec{b} = \frac{1}{2}[1\ \bar{1}\ 0]$ occur. They are more strongly bowed-out, with some being half loops originating at the interfaces. While the screw parts of

Fig. 4. Dislocations that have moved during in situ deformation of material with nearly lamellar microstructure at room temperature imaged after unloading. $(\bar{1}\ \bar{1}\ 1)_\gamma$ interfaces close to edge-on. For $\vec{b}$ see Thompson tetrahedron inserted, $\vec{g} = [1\ \bar{1}\ \bar{1}]$.

Fig. 3. Dislocations and twins under load during in situ deformation of near-gamma Ti-Al at room temperature. (a) Ordinary dislocations with $\vec{b} = \frac{1}{2}[\bar{1}\ \bar{1}\ 0]$, slip plane $(1\ \bar{1}\ 1)$, $\vec{g} = [\bar{1}\ \bar{1}\ 1]$. (b) Superdislocations with $\vec{b} = [0\ \bar{1}\ \bar{1}]$, slip plane $(1\ \bar{1}\ 1)$, $\vec{g} = [\bar{1}\ 11]$. (c) All dislocations in contrast, $\vec{g} = [\bar{2}\ 02]$. (d) Schematic drawing illustrating the relative orientations of matrix and twin by means of (from top to bottom): diffraction pattern (twin reflections indicated in italics, pure twin reflections as ring), elementary cells (slightly tilted for clarity, atom sizes reduced), and corresponding Thompson tetrahedra isolated with occurring Burgers vectors indicated ($\vec{b} = \frac{1}{2}[\bar{1}\ \bar{1}\ 0]$—full arrow, $\vec{b} = [0\ \bar{1}\ \bar{1}]$—empty arrow), respectively.

the superdislocations lie parallel to the image plane the ordinary dislocations are inclined, which is indicated by the shape of the arrow. Both types of dislocations are pinned as in the near-gamma material, and again debris has formed. In addition, dislocations with Burgers vector $\vec{b}=\frac{1}{2}[11\,\bar{2}]$ occur which are parallel to the trace of the interface. In a neighbouring lamella crossing straight dislocations appear in a high density. In many lamellae, ordinary dislocations are dominating as shown in Fig. 5. All features of dislocation dynamics are similar to the near-gamma material, i.e. the bowing-out between obstacles, the average obstacle distance of about 0.15 μm, and the jerky mode of dislocation motion.

In contrast to coarse grained Al-rich single phase materials, the deformation properties of the two-phase materials are significantly affected by the large number

Fig. 5. Dislocation structure under load during in situ deformation of nearly lamellar Ti-Al at room temperature. $\{111\}_\gamma$ interfaces are imaged nearly edge-on. Ordinary dislocations are imaged. For the Burgers vector see the Thompson tetrahedron inserted.

of different interfaces. This may be illustrated by the effect of a narrow twin lamella on the dislocation motion. Fig. 3 shows such a defect oriented edge-on and separating the lower right corner from the rest of the figure. As outlined in the Thompson tetrahedra in Fig. 3(d) the interfaces are barriers for the dislocation motion. The Burgers vector $[0\,\bar{1}\,\bar{1}]$ of the superdislocations does exist in both the twin lamella and the matrix left and right of it, however, the $\frac{1}{2}[\bar{1}\,\bar{1}\,0]$ Burgers vector of the ordinary dislocations does not. Thus, ordinary dislocations move independently left and right of the twin lamella, whereas two superdislocations are visible which easily penetrate the twin and extend on either side of it without deflection (marked by arrows in Fig. 3(b)). This behaviour demonstrates that generally the interfaces are very effective barriers for the dislocation motion. In materials of nearly lamellar microstructure as in Fig. 4, only few dislocations extend beyond the interfaces. This is true for even large stresses in the vicinity of a crack as e.g. in this figure, with its distance to the crack being less than 10 μm.

3.2. Deformation at 900 K

The typical feature of dislocations in the near-gamma microstructure at high temperatures is displayed in Fig. 6(a–c), reproducing micrographs of a diffraction contrast experiment taken after unloading at room temperature. Ordinary dislocations (a slip band) and superdislocations are imaged individually in (a) and (b) and together in (c). They all have moved on the same type of slip plane (see inset). The ordinary dislocations with $\vec{b}=\frac{1}{2}[1\,\bar{1}\,0]$ are mainly of screw type originally, showing a bowed-out shape, a situation similar to that during room temperature deformation. Stereo pairs taken from other specimen areas, however, show that the arrangements are not planar but contain helical paths. The pinning agents are all jogs. Each bowed-out segment lies on a different plane with a unique sense of the jogs forming a stair-like configuration. In contrast to that, superdislocations of $\vec{b}=[0\,\bar{1}\,1]$ are characterised by rather straight segments of preferred screw and edge orientations. Fig. 7 represents another example of superdislocations of $\vec{b}=\langle 101]$ with segments strictly oriented in screw direction as well as a number of helical arrangements.

In the nearly lamellar microstructure, the predominating ordinary dislocations are smoothly bent with large radii of curvature as in Fig. 8. The $\langle 101]$ direction seems to be a preferred orientation of these dislocations. Dislocation debris appears in the form of small dislocation loops, not as dipoles as at room temperature. Superdislocations of $\vec{b}=\langle 101]$ have almost

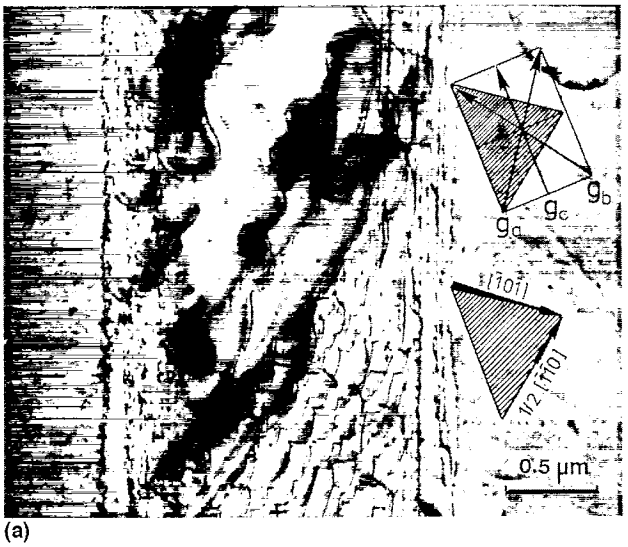

(a)

(b)

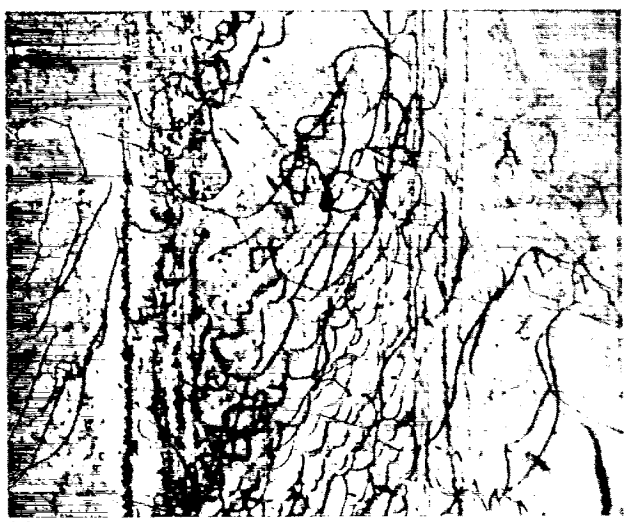

(c)

Fig. 6. Microstructure of near-gamma Ti-Al during in situ deformation at 900 K. (a) Ordinary dislocations with $\vec{b} = \frac{1}{2}[1\ \bar{1}\ 0]$ in contrast. (b) Superdislocations with $\vec{b} = [0\ \bar{1}\ 1]$ in contrast. (c) All dislocations in contrast.

straight segments oriented in crystallographic directions (Fig. 9).

The striking feature in both the near-gamma and the nearly lamellar microstructures is the instantaneous generation of a large number of dislocations, if the load is gradually raised. Afterwards, the dislocation motion is viscous around 900 K. Unfortunately, in most of the high-temperature in situ experiments the character of moving dislocations could not be determined so that it is not clear whether these statements about the dynamic behaviour apply to both the ordinary dislocations and superdislocations.

The results reported in Section 3.1 and regarding the importance of interfaces for dislocations and twins also apply to deformation temperatures of 900 K. The motion of the majority of dislocations and the twinning processes are restricted to single grains or lamellae as have been realised by post mortem studies performed on materials of similar composition and microstructure [3,22]. In the nearly lamellar microstructure semicoherent interfaces act as efficient dislocation sources especially in the vicinity of cracks. In this way, the number of dislocations can effectively be raised resulting in crack tip shielding. Fig. 10 presents such an example. Emission of perfect and twinning dislocations from mis-match structures of lamellar interfaces has also been observed by TEM in situ heating studies and post mortem investigations of deformed material [14,22,23].

3.3. Fracture processes at room temperature and 900 K

Cracks in the near-gamma microstructure do not always have crystallographically oriented edges as in Fig. 1. In many cases they are curved, especially after nucleation in highly distorted zones. On the other hand, cracks are also aligned along {111} planes, but then they have again deflected from this orientation. The number of cracks covering more than two or three grains is small. In many cases new cracks nucleate in front of the main crack. Sometimes bridges remain hindering the easy extension of the cracks even in this microstructure. Obviously, α_2 triple junctions are able to impede cracks. In a video sequence, a crack approached such an α_2 grain, stopped in front of the interface, and finally moved around the grain.

In the nearly lamellar microstructure, cleavage is a very frequent failure mechanism. The cleavage faces are of {111} type, i.e. the crack often changes its direction on moving from lamella to lamella (Fig. 2) so that a much more tortuous crack path is formed. However, the lamella interfaces are {111} planes, too, so that the cracks often run along the interfaces, not only at an inconvenient tensile axis. Dense groups of intersecting microtwins sometimes lead to crack nucle-

ation as evidenced for single phase TiAl in [10]. On the other hand, twinning contributes to crack shielding like dislocation plasticity. Frequently, new cracks form in front of the main crack so that the remaining ligaments bridge the actual crack tip as in the near-gamma material.

4. Discussion

The motion of individual dislocations in the γ phase of both the two-phase alloys of the present study is generally very similar to that in the single-phase γ material investigated earlier [8–10].

Several aspects of the glide resistance described here have also been deduced from estimations of activation parameters and post mortem studies performed on the same material [14,15]. At room temperature, ordinary dislocations dominate. They are pinned at localised obstacles and jogs. In the two-phase materials, the obstacle distance of 0.15 μm is slightly larger than that in the aluminium-rich material (0.1 μm). It is argued in [8,9] that small oxide precipitates act as localized obstacles, although these precipitates have not yet been unequivocally proved. It is well known [28], however, that the deformation parameters of Ti-Al alloys depend on the oxygen content. The increased obstacle distance in the two-phase materials should then result from the presence of the α_2 phase, which getters oxygen. The dynamic behaviour, i.e. the details of the mode of the jerky motion of dislocations described in [8], strongly supports precipitation hardening as a mechanism, controlling the dislocation mobility. The alignment of most of the ordinary dislocations in screw orientation as well as the fact that the dislocation bowing does practically not relax after unloading may point to the additional action of a lattice friction mechanism.

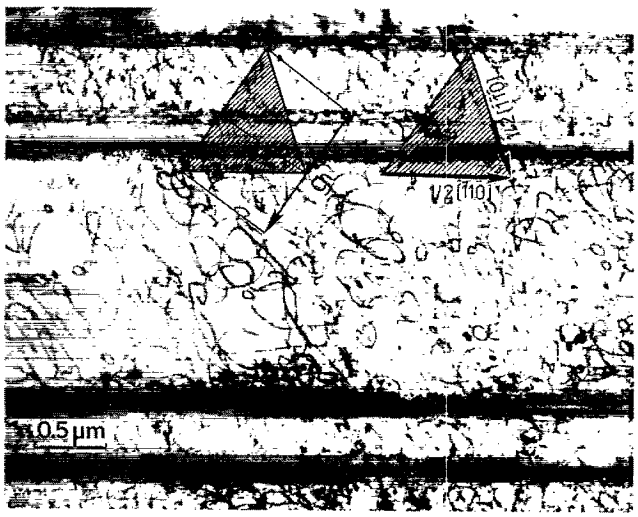

Fig. 8. Dislocation structure in nearly lamellar Ti-Al under load during in situ deformation at 900 K. Most dislocations are ordinary dislocations.

Fig. 7. Microstructure of near-gamma Ti-Al during in situ deformation at 900 K. Most dislocations are superdislocations.

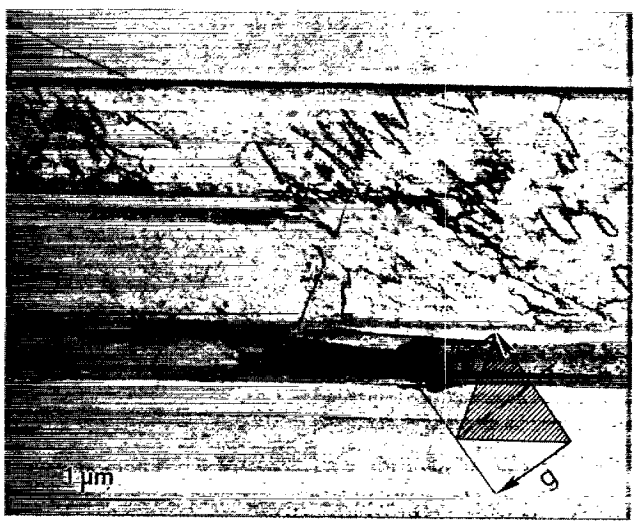

Fig. 9. Dislocation structure under load during in situ deformation of nearly lamellar Ti-Al at 900 K. Superdislocations are imaged.

Fig. 10. Dislocation structure in nearly lamellar Ti-Al after unloading an in situ specimen deformed at 900 K. Multiplication processes (arrow) at interface dislocations at the site of a former lamella (L), which receded during thermal treatment.

The macroscopic yield stress of the Al-rich Ti–Al alloy could semiquantitatively be understood by the superposition of precipitation hardening and the long-range interaction between dislocations. In addition, the obstacle distance is well consistent with the activation volume measured by stress relaxation experiments [8]. In the two-phase alloys, the activation volume is much smaller [14,15]. This difference again hints at the action of a lattice friction mechanism. At room temperature superdislocations generally show a behaviour similar to that of ordinary dislocations. The smaller bowout of superdislocations is due to the much higher line tension. The yield stress of the two-phase alloys is remarkably higher than that of the pure γ material, which might be due to the influences of the microstructure, to grain boundaries and interfaces between the lamellae in the nearly lamellar Ti–Al.

The similarity between the dislocation behaviour in γ single-phase and two-phase Ti–Al extends also to high temperatures. As described for the γ material in [8,9], the curly shape disappears. The ordinary dislocations are smoothly bent and occur in nonplanar arrangements. The pronounced formation of helical structures observed in the two-phase alloys has not been observed so clearly in the single phase γ crystals. These structures must have been formed by climb superimposed onto the glide motions. Similar structures have already been observed during in situ heating studies on a Ti-48at.%Al-2at.%Cr alloy with a lamellar microstructure [13]. The helices and the stair-like arrangement of the dislocation bow-outs in the near-gamma TiAl point to unidirectional climb motions. The nature of the point defects involved in dislocation climb could not be identified. However, of the various defects which can exist in γ Ti–Al the vacancy is the only species that is always present in appreciable concentrations even in thermodynamic equilibrium. The two-phase materials used in the present study can become more defective for mainly two reasons. Firstly, excess vacancies may result from the rapid quenching after the thermal treatments described in Section 2. Order of magnitude estimates show that the climb velocities observed in Ti–Al in [14] are consistent with a relatively low excess vacancy concentration of $c/c_0 = 1.3...5$ [24] and the diffusion coefficients determined in [29]. Secondly, under the experimental conditions used in the present study excess vacancies can also be produced by irradiation with high-energy electrons. Since the acceleration voltage used (1000 kV) is well above the threshold voltage for Ti and Al, displacement defects can be produced and may precipitate out in form of discs on close-packed planes. However, the helices and loops observed appear only in connection with dislocation movement. Besides, similar defect structures have also been observed during TEM in situ heating studies performed at 120 and 200 kV [13,14], where radiation damage is less likely to occur. Furthermore, activation parameters estimated on the same two-phase materials have indicated that at deformation temperatures higher than 900 K dislocation climb may occur [13,14] so that the present observations do not seem to be an artefact of the in situ deformation technique.

The $\langle 101]$ superdislocations have preferentially screw character. The preferred orientations of superdislocations are in agreement with the locking mechanisms usually discussed (e.g. in [11]). In the present study, also ordinary dislocations align preferentially in $\langle 101]$ directions. Generally, the preferred alignment of dislocation segments in $\langle 110]$ directions has been suggested to occur by a non-planar dissociation on oblique $\{111\}$ planes [14].

At high temperatures, the dislocations show quite a peculiar dynamic behaviour. During careful loading a great number of dislocations is generated instantaneously like in an avalanche. This was already observed in single phase γ material [8,30]. On further loading, the

dislocations do not move again, or they move in a viscous manner. The viscous dislocation motion at high temperatures is not a general phenomenon occurring in other materials. Usually, viscous motion is connected with lattice friction mechanisms at low temperatures like the Peierls mechanism. With increasing temperatures, the motion becomes jerky, e.g. owing to localised obstacles as observed in TiAl at room temperature. In many materials, at high temperatures, the deformation assumes an athermal character which is accompanied with dislocations jumping over distances of the order of the dislocation spacing, or larger. However, a viscous motion at high temperatures was also proved by in situ straining experiments on Ni–Al [31]. It is most certainly connected with diffusion processes controlling the dislocation mobility at high temperatures and might be a more general phenomenon of intermetallic alloys. This is in accordance with the observation of climb described above. Besides, the TiAl alloys show a strain ageing behaviour, particularly at intermediate temperatures [14,23,32]. Strain ageing can be explained by the formation of point defect atmospheres around the dislocations, where the latter may experience frictional forces and viscously move at intermediate velocities, however move freely at high velocities like in the avalanche during the first loading.

The results of the present in situ experiments show, in accordance with [8], that the anomalous deformation behaviour of the Ti–Al alloys cannot be explained solely on the basis of the properties of superdislocations. The processes are much more complex, requiring further experiments for a deeper understanding. The higher flow stress of the two-phase alloys and the differences in the fracture behaviour between the near-gamma and the nearly lamellar materials are certainly not due to intrinsic dislocation behaviour, but to the particular microstructures. As observed also in the in situ experiments, the interfaces are very effective barriers to the dislocation motion. Several aspects of the glide resistance described here have also been deduced from estimations of activation parameters and post mortem studies performed on the same material [14,15]. The {111} interfaces play an important role during the fracture processes. Cleavage-like fracture on {111} planes has already been revealed by conventional and high resolution TEM studies [21]. In order to follow the main crack direction, the crack front has frequently to be deflected. It has been speculated in [21] that this is a significant toughening mechanism in lamellar Ti–Al, which contributes to the relatively high fracture toughness compared with the near-gamma structures.

Acknowledgements

The authors are indebted to the staff of the Halle HVEM for the continuously proper condition of the microscope. Financial support by the Deutsche Forschungsgemeinschaft is gratefully acknowledged.

References

[1] D.M. Dimiduk, in: Y.-W. Kim, R. Wagner, M. Yamaguchi (Eds.), Gamma Titanium Aluminides, TMS, Warrendale, PA, 1995, p. 3.
[2] L. Zaho, K. Tangri, Philos. Mag. A 65 (1992) 1065.
[3] F. Appel, P.A. Beaven, R. Wagner, Acta Metall. Mater. 41 (1993) 425.
[4] V.K. Vasudevan, M.A. Stuecke, S.A. Court, H.L. Fraser, Phil. Mag. Lett. 59 (1989) 299.
[5] S. Farenc, D. Calliard, A. Couret, Proc. 6th Int. Symp. on Intermetallic Compounds, Structure and Mechanical Properties, Tokyo, 1991, p. 791.
[6] S. Farenc, A. Couret, in: I. Baker, R. Darolia, J.D. Whittenberger, M.H. Yoo, High-Temperature Ordered Intermetallic Alloys V, Mater. Res. Soc. Proc. 288, Pittsburgh, PA, 1993, p. 465.
[7] S. Farenc, A. Coujou, A.A. Couret, Philos. Mag. A 67 (1993) 127.
[8] D. Häussler, U. Messerschmidt, M. Bartsch, M. Aindow, I.P. Jones, in preparation.
[9] U. Messerschmidt, M. Bartsch, D. Häussler, M. Aindow, R. Hattenhauer, I.P. Jones, in: J.A. Horton, J. Baker, S. Hanada, R. D. Noebe, D.S. Schwartz (Eds.), High-Temperature Ordered Intermetallic Alloys VI, MRS Symp. Proc., vol. 364, MRS, Pittsburgh, PA, 1995, p. 47.
[10] D. Häussler, M. Bartsch, U. Messerschmidt, M. Aindow, I. P. Jones, in: Inst. Phys. Conf. Ser. 147 (Sec. 11), Proc. EMAG Conf. Birmingham, 1995, p. 463.
[11] G. Hug, A. Loiseau, P. Veyssière, Philos. Mag. A 57 (1988) 499.
[12] G. Hug, J. Phan-Courson, G. Blanche, Mater. Sci. Eng., A 192/193 (1995) 673.
[13] F. Appel, U. Lorenz, U. Sparka, R. Wagner, in: K. Oikawa, M. Maruyama, S. Takeuchi, M. Yamaguchi (Eds.), Strength of Materials, Proc. ICSMA 10, The Japan Institute of Metals, Sendai 1994, p. 341.
[14] F. Appel, U. Lorenz, M. Oehring, U. Sparka, R. Wagner, Mater. Sci. Eng. A, 233 (1997) 1.
[15] F. Appel, U. Sparka, R. Wagner, in: J.A. Horton, J. Baker, S. Hanada, R.D. Noebe, D.S. Schwartz (Eds.), High-Temperature Ordered Intermetallic Alloys VI, MRS Symp. Proc., vol. 364, MRS, Pittsburgh, PA, 1995, p. 623.
[16] M. Yamaguchi, H. Inui, in: R. Darolia, J.J. Lewandowski, C.T. Liu, P L. Martin, D.B. Miracle, M.V. Nathal (Eds.), Structural Intermetallics, TMS, Warrendale, PA, 1993, p. 127.
[17] Y.-W. Kim, in: Y.-W. Kim, R. Wagner, M. Yamaguchi (Eds.), Gamma Titanium Aluminides, TMS, Warrendale, PA, 1995, p. 637.
[18] K. Kishida, D.R. Johnson, Y. Shimada, H. Inui, Y. Shirai, and M. Yamaguchi, in: Y.-W. Kim, R. Wagner and M. Yamaguchi (Eds.), Gamma Titanium Aluminides, TMS, Warrendale, PA, 1995, p. 219.
[19] K.S. Chan, Y.-W. Kim, Metall. Trans. A 25 (1994) 1217.
[20] F. Appel, U. Lorenz, T. Zhang, R. Wagner, in: J.A. Horton, J. Baker, S. Hanada, R.D. Noebe, D.S. Schwartz (Eds.), High-Temperature Ordered Intermetallic Alloys VI, MRS Symp. Proc., vol. 364, MRS, Pittsburgh, PA, 1995, p. 493.
[21] F. Appel, U. Christoph, R. Wagner, Philos. Mag. A 72 (1995) 341.

[22] F. Appel, R. Wagner, in: M.H. Yoo, M. Wuttig (Eds.), Twinning in Advanced Materials, TMS Warrendale, PA, 1994, p. 317.
[23] F. Appel, R. Wagner, in: Y.-W. Kim, R. Wagner, M. Yamaguchi (Eds.), Gamma Titanium Aluminides, TMS, Warrendale, PA, 1995, p. 231.
[24] F. Appel and R. Wagner, to be published.
[25] U. Messerschmidt, F. Appel, Ultramicroscopy 1 (1976) 223.
[26] U. Messerschmidt, M. Bartsch, Ultramicroscopy 56 (1994) 163.
[27] H. Inui, M.H. Oh, A. Nakamura, M. Yamaguchi, Philos. Mag. A 66 (1992) 539.
[28] S.C. Huang, E.L. Hall, Metall. Trans. A, 22 (1991) 427.
[29] S. Kroll, H. Mehrer, N. Stolwijk, Ch. Herzig, R. Rosenkranz, G. Frommeyer, Z. Metallkunde 83 (1992) 591.
[30] A. Couret, private communication, 1996.
[31] R. Haushälter, M. Bartsch, U. Messerschmidt, Mater. Sci. Eng. A, Proc. ICSMA-II, Prague 1997, in press.
[32] M.A. Morris, T. Lipe, D.G. Morris, Scripta Mater. 34 (1996) 1337.